

**TUBE SHEET STRUCTURAL ANALYSIS OF INTERMEDIATE HEAT EXCHANGER
FOR FAST BREEDER REACTOR "MONJU"**

INTERNATIONAL ATOMIC ENERGY AGENCY

Specialist's Meeting on Advances in Structural Analysis for LMFBR Applications

Paris, France

11 - 15 Oct. 1982

Y. Nakagawa (Hitachi works, Hitachi, Ltd.)
T. Ueno (Hitachi works, Hitachi, Ltd.)
Y. Fukuda (Mechanical Engineering Lab., Hitachi, Ltd.)
M. Ichimiya (Power Reactor and Nuclear Fuel Development Corp.)

-218-



XA0201728

Tube Sheet Structural Analysis of Intermediate Heat Exchanger
for Fast Breeder Reactor "Monju"

Y. Nakagawa*
T. Ueno**
Y. Fukuda***
M. Ichimiya†

Abstract

The Prototype Fast Breeder Reactor "Monju" is the first power generating fast breeder reactor in Japan. We have been designing the components of the plant for manufacturing. Among these is the intermediate heat exchanger (IHX) which exchanges heat between primary and secondary sodium loop.

The tube sheet of IHX (shell to ligament junction) is a difficult area from the view point of structural strength design under elevated temperature.

To validate the structural integrity of tube sheet we performed the series of inelastic analysis and tube sheet thermal shock test using test pieces and half scale model of actual design.

The results of inelastic analyses showed there is little progressive deformation around shell to ligament structural discontinuous junction.

Furthermore, thermal shock tests showed no increase of an accumulative deformation.

By these analyses and experiments, structural reliability of tube sheet could be shown.

* Senior Engineer ; Advanced Reactor Dept., Hitachi Works, Hitachi, Ltd.
** Advanced Reactor Dept., Hitachi, Works, Hitachi, Ltd.
*** Senior Researcher; Mechanical Engineering Research Lab., Hitachi, Ltd.
† Power Reactor and Nuclear Fuel Development Corp.

1. Introduction

The prototype Fast Breeder Reactor "Monju" is the first power generating fast breeder reactor in Japan. We have been designing the components of the plant for manufacturing. Among these is the intermediate heat exchanger (IHX) which exchanges heat between primary and secondary sodium loop.

The tube sheet of IHX (shell to ligament junction) is a difficult area from the view point of structural strength design under elevated temperature.

To validate the structural integrity of tube sheet we performed the series of inelastic analysis and tube sheet thermal shock test using test pieces and half scale model of actual design.

2. Structure of IHX and stress generating mechanism

Fig. 1 shows the bird eye view drawing of Monju IHX. It has upper and lower tube sheets and about 3000 heat transfer tubes under liquid sodium environments. Primary sodium flows outside tubes and secondary one goes through straight tubes. Diameter of a cylindrical shell is about 3,000mm and total height is about 13,300mm.

Fig. 2 explains stress generating mechanism around the upper tube sheet.

The tube sheet consists of two major parts; one is "Ligament", perforated thick plate and another is "Shroud", thin conical shell. When primary sodium temperature goes down, as such in manual trips of the plant, first, primary sodium temperature outside shroud decreases.

This primary sodium flows in outside tubes and then secondary sodium temperature goes down and flows through holes in ligament. Because the ligament has so many holes for secondary sodium, its average temperature quickly follows that of secondary sodium. This causes temperature difference between the ligament and the shroud. This temperature difference, in turn, causes high stresses around tube sheet shell junction.

In case of Monju IHX tube sheet, an evaluation on progressive deformation is a main concern.

To validate structural reliability, experiments and inelastic analyses have been done.

3. Simple tests using plate specimens

3.1 Methods of tests

To know the stress and strain behavior, first fatigue tests using simple plate specimens described in Fig. 3 have been performed.

Fig. 4 shows test devices with a specimen. Testing conditions are shown in Table 1.

Material of specimen is 304SS, same as actual IHX.

Stress state of this type specimen, is obviously different from that of an actual IHX where the effects of hoop stresses can not be negligible.

In spite of this difference with an actual component we believe it is useful to get the basic information of concerned area.

We put thermocouples, strain gauges and dial gauges to obtain necessary data of specimen's behavior.

3.2 Results of tests

Fig. 5 shows the relation between accumulative strain and repeated cycles of forced deflection.

These data imply we have a limit above which strain continuously increases, i.e. the limit for progressive deformations.

4. Half scale model tests of tube sheet

4.1 Test apparatus

Fig. 6 shows the test apparatus used in this experimental investigation. It is made of 304SS. The outer diameter of the tube sheet is about 1000mm and thickness is 100mm. The thickness of shroud is 16mm. Tests were performed at 550°C

maximum. Electric heater was used to heat up, and air induced from lower side of the tube sheet was used to cool down. Temperature difference between the tube sheet and shroud can be controlled by adjusting heater power or inducing air.

Since the tube sheet has a lot of perforation, this temperature drops faster than shell when air is induced. Experiments were carried out controlling average temperature difference between the tube sheet and shell as parameters. This average temperature difference is defined positive when shell temperature is higher than plate temperature.

In these experiments, temperature control is very important. 47 thermocouples are set on whole test apparatus to observe its temperature and the electric heater is divided into several blocks and each block of heater can be controlled independently.

15 high temperature strain gauges are set mainly at the highest stress generating point obtained by prior stress analyses. Since the length of strain gauge is about 20mm, there is probability these gauges can't pick up the maximum value of strain. However, comparison of strain is performed between these high temperature strain gauge and adhesive type gauge, whose length is 5mm, which is allowed to use under 300°C and comparison between experiments and analysis was made. Suitable adjustments was made considering these comparisons.

Tests were finished when ΔT becomes a certain value determined in advance. During the tests temperature and strain are recorded continuously.

4.2 Test Condition

Table 2 shows the list of test conditions. Test 1 - 6 are carried out mainly to check characteristic behavior of high temperature strain gauge and temperature control method. In test 11 and 12 ΔT equals 160°C and 250°C respectively and temperature of the tube sheet was always lower than that of shell. In the following tests except test 14 temperature difference changes from plus to minus that is stress around junction changes from tension (compression) to compression (tension).

These tests are carried out to verify experimentally whether loading cycle condition (zero-tension, zero-compression, tension-compression) has something to do with strain hysteresis around the junction.

Table 3 shows the maximum stress calculated by elastic analyses based on temperature distributions for respective test conditions.

Allowable stress for S_n (primary plus secondary stress intensity range) and S_n' (S_n minus thermal bending stress) is 29 kg/mm^2 . S_n exceeds the allowable value when ΔT is over 150°C and S_n' exceeds it when ΔT is over 275°C . Therefore S_n exceeds the allowable value in test 11 and both S_n and S_n' exceed the allowable value in Test 11 and 16 although we have another design method when S_n exceeds 35 m .

4.3 Test Results

(1) Relation between temperature difference range ΔT and strain range

Fig. 7 shows the relation between temperature difference range and maximum strain range obtained by these experiments. Where ΔT is under about 60°C , it shows elastic behavior and the relation is linear. Where ΔT is over 60°C , increase of strain range becomes gradually larger caused by effect of plasticity. Where ΔT is under 300°C , load cycle is given to one direction (Zero-tension). On the other hand where ΔT is over 300°C , this is given to both directions (tension-compression). In this figure in the region where ΔT is near 300°C , the curve is smooth and this figure shows it is appropriate to use ΔT as a parameter for arranging strain range.

(2) Strain loop

Figs. 8 and 9 show relation between temperature difference ΔT and strain in each cycle of Test 11 ($\Delta T = 250^\circ\text{C}$ and zero-tension condition) and Test 16 ($\Delta T = 400^\circ\text{C}$ and tension-compression) respectively. These figures correspond to Figs. 11, 12 and 13 which show the analytical results. In test 11 and test 16, 10 times and 5 times repeated loading was given respectively. In both tests,

however, ΔT strain loops was quite stable. By the fatigue damage evaluation using measured strain range Df becomes 0.056.

5. Non Linear Analyses

5.1 Elastic analyses

Elastic analyses by FEM were made using temperature distribution which is measured in experiments. 2 cases of elastic analyses were carried out. Maximum stress values on inner surface at structural discontinuity were obtained by these analyses.

Since it is found that stress is proportional to ΔT from the results of tests 6 and 11, the maximum value in test 16 is extrapolated from the values of tests 6 and 11. Since the restriction of S_n and S_n' is required to evaluate fatigue damage in ASME Code, in these cases fatigue damage evaluation by ASME code is not applicable. In spite of this, fatigue damage evaluation was carried out and shows $Df = 2.66$, which exceeds allowable value 1.0 to a great extent. Comparing this value with that of calculated based on experimental data before, we find the evaluation on an elastic basis is very conservative.

5.2 Non-linear analyses

Seven cases of non-linear analyses were performed as tabulated on Table-4. To save computing time we used a partial model by forced deflection instead of a full model and thermal loading respectively. Fig. 10 shows the in elastic analysis model. Figs. 11, 12 and 13 are the stress and strain relations for cases 1, 4 and 5 respectively.

Fig. 11 shows stress strain relation when loading condition is zero-tension, whose value of strain is equivalent to $\Delta T = 300^\circ\text{C}$. Fig. 12 shows stress strain relation for tension-compression, whose value is equivalent to $\Delta T = 500^\circ\text{C}$. Fig. 13 is the case of additional creep to case 4. In case that zero-tension load cycle is given, strain increases slightly by repetition of forced displacement even though the

-221-

amount is very small compared to allowable limits. Fig. 14 shows detail non-linear behaviors of stresses and strains around shell to tube sheet junction.

6. Conclusion

Evaluation of behavior in structural discontinuity at tube sheet under elevated temperature was performed by component tests and analyses.

In case of high "Primary + Secondary stress range S_n ", analyses show strain increases continuously under zero-tension loading conditions even though the amount is very small and no increases for tension-compression. By half scale model tests, however, no increases of strain could be found for both types of loading.

-222-

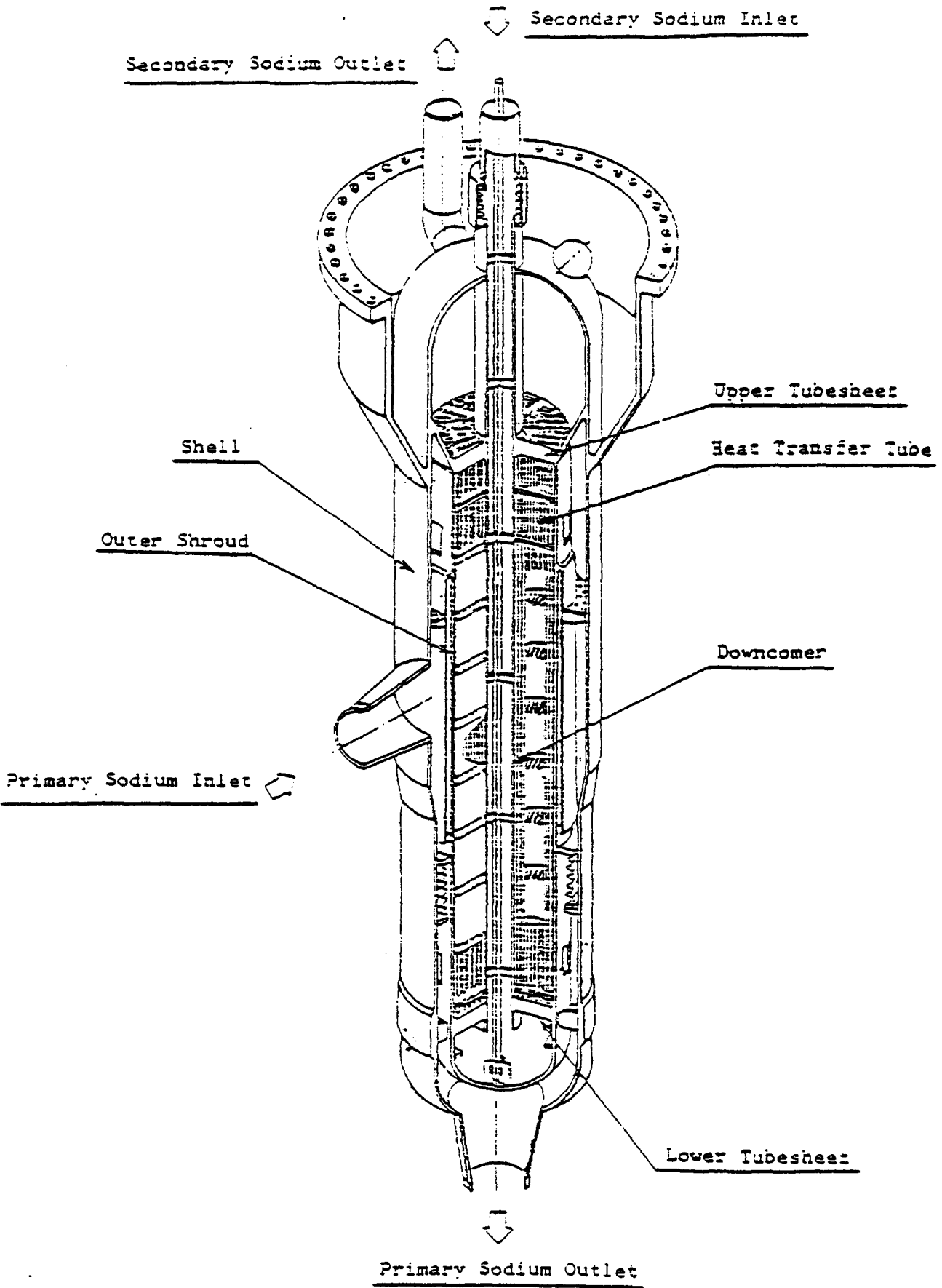


Fig. 1 "MONJU" Intermediate Heat Exchanger

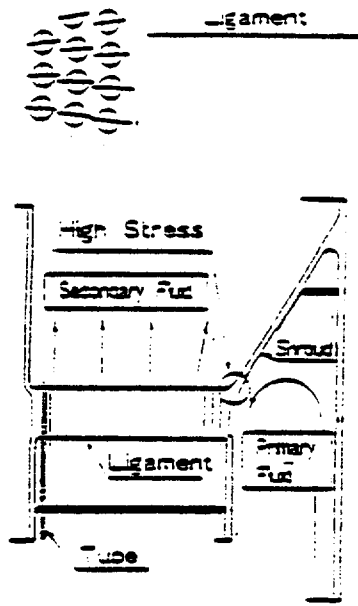


Fig. 2 Stress generation mechanism in tubesheet

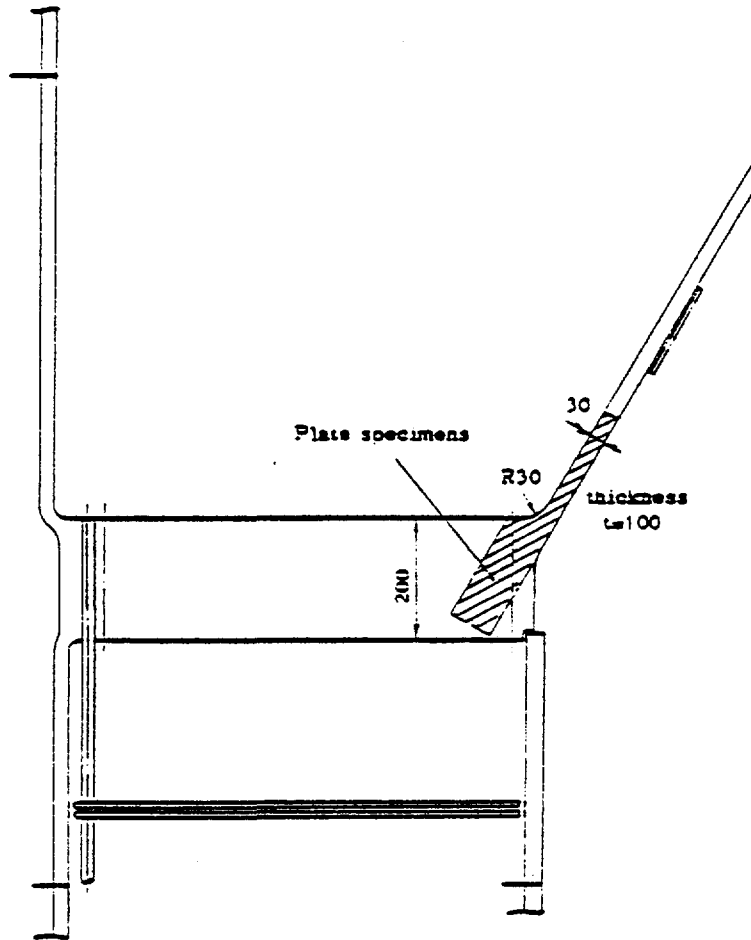


Fig. 3 Plate specimens for fatigue tests

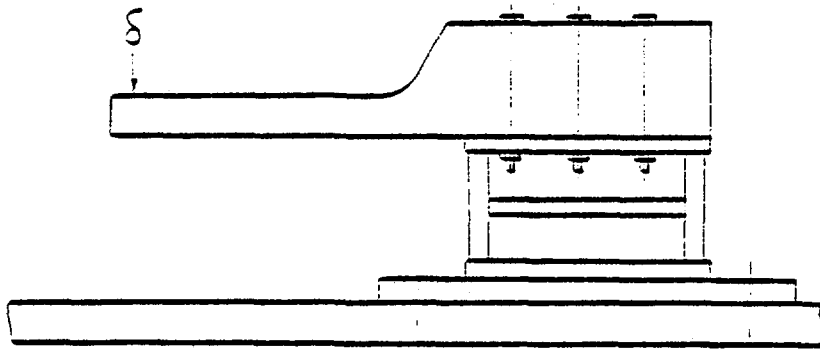


Fig. 4 Test devices for glass specimens

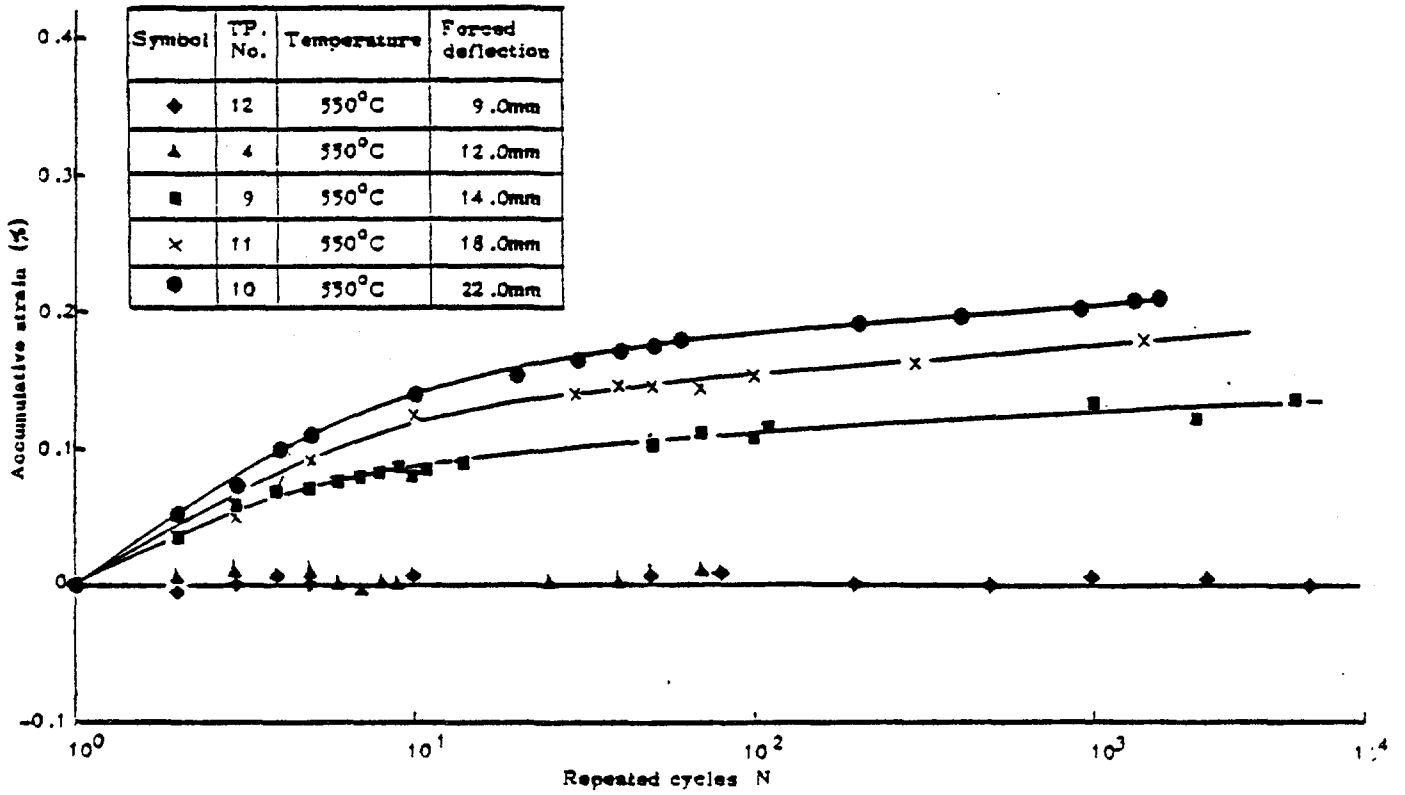


Fig. 5 Accumulative strain

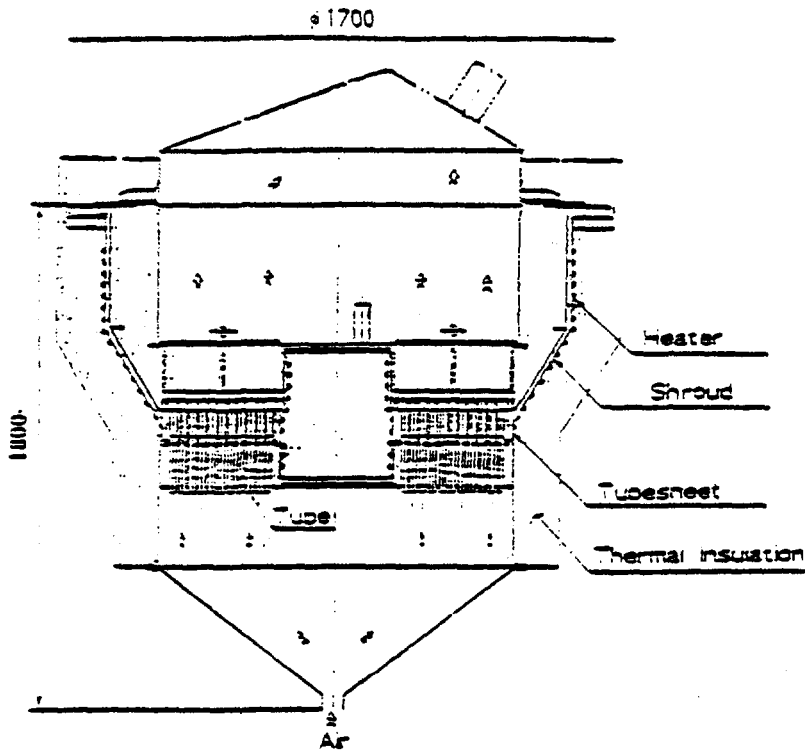


Fig. 6 Tubesheet thermal shock test facility

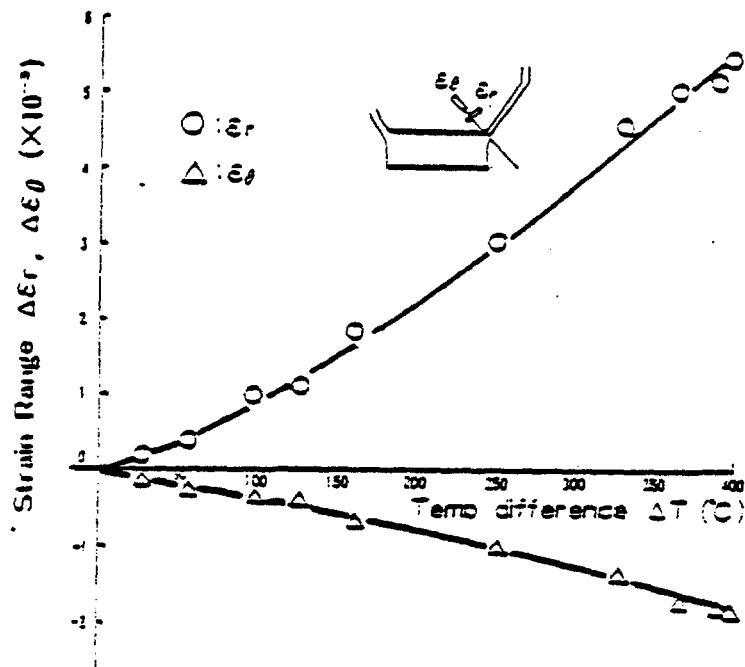


Fig. 7 Maximum strain range

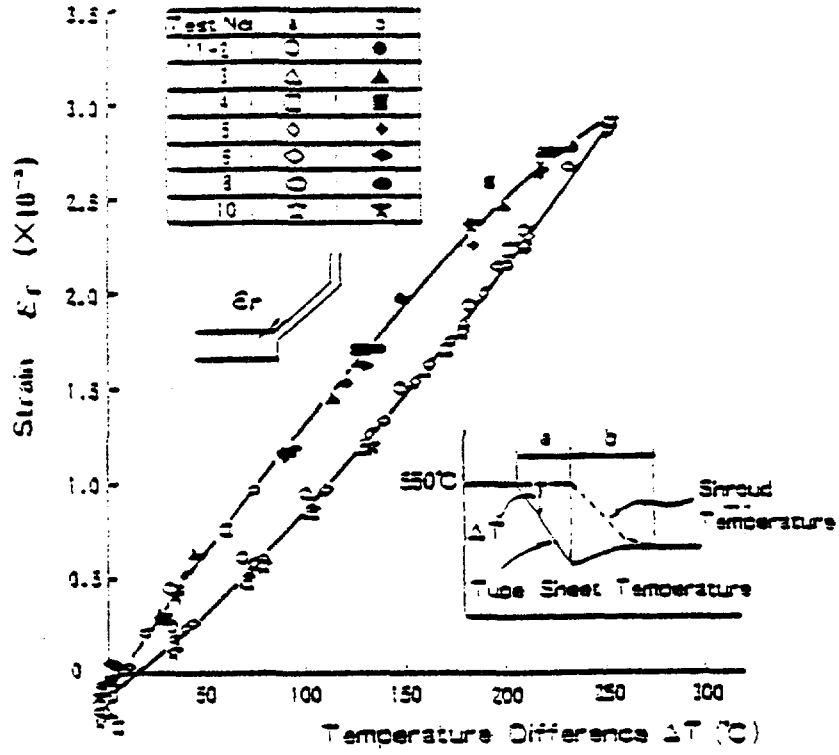


Fig. 8 Relation between temperature difference and strain

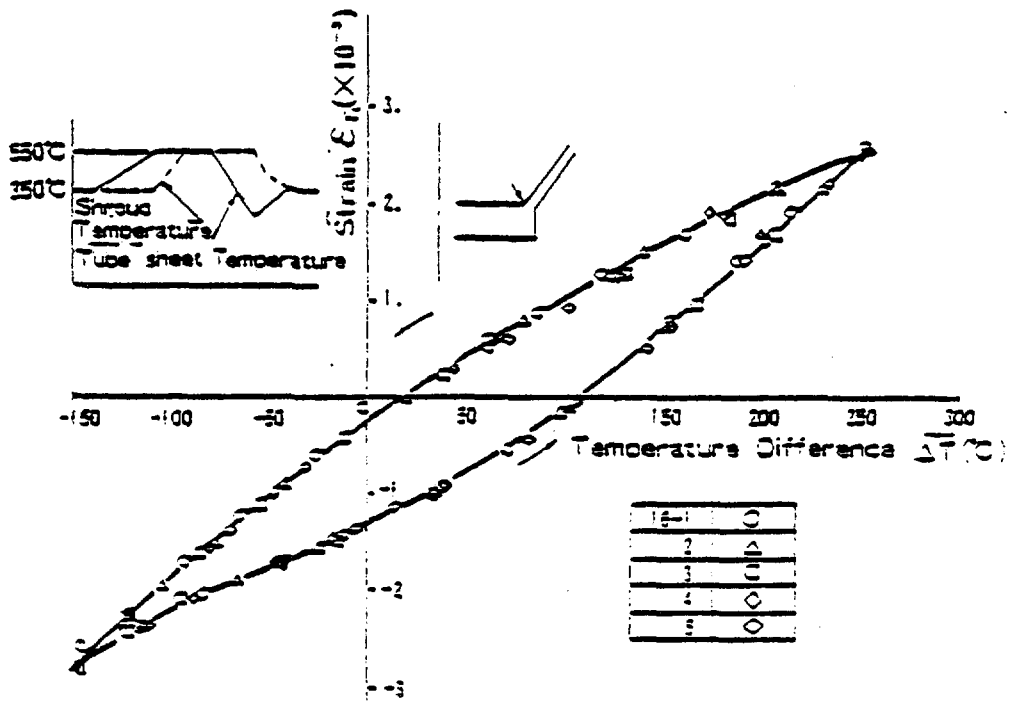


Fig. 9 Relation between temperature difference and strain

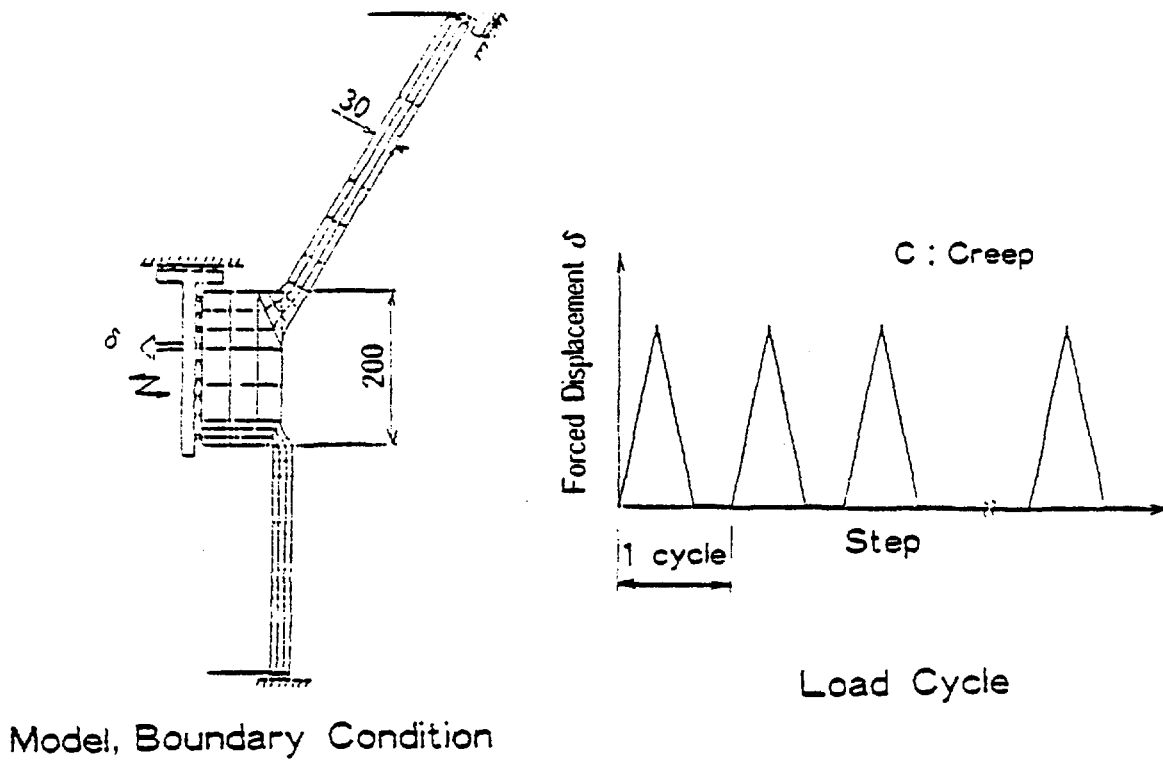


Fig. 10 Inelastic analysis by partial model

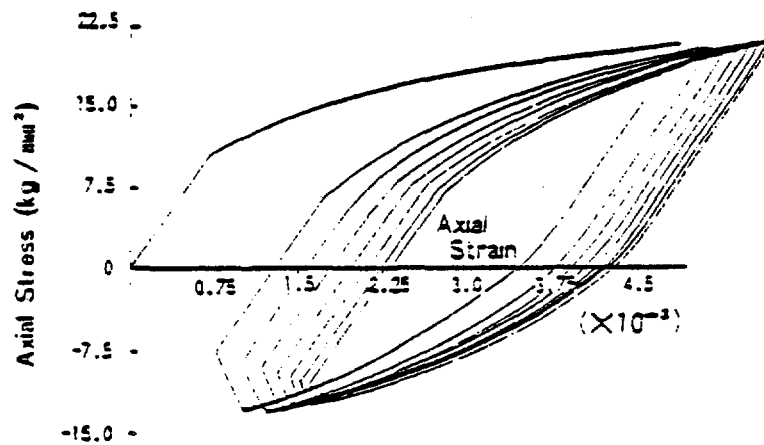


Fig. 11 Stress-strain curve case 1

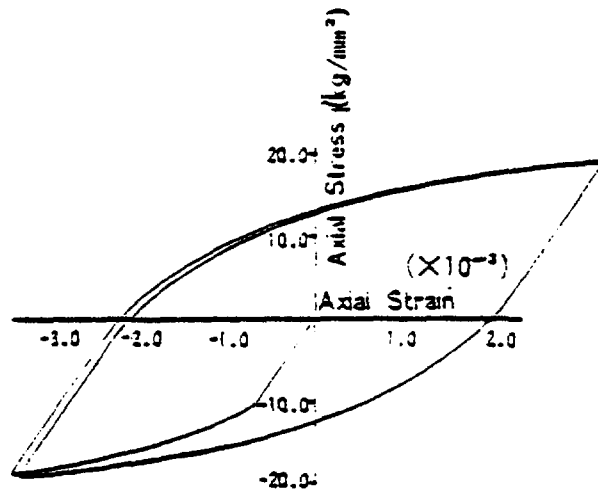


Fig. 12 Stress-strain curve case 4

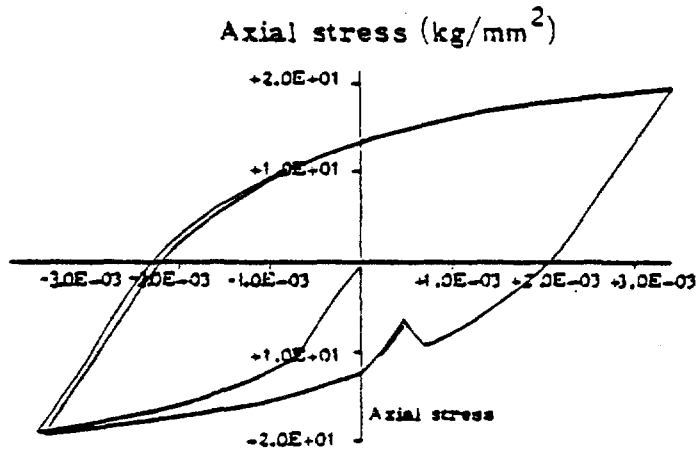


Fig. 13 Stress-strain curve case 5

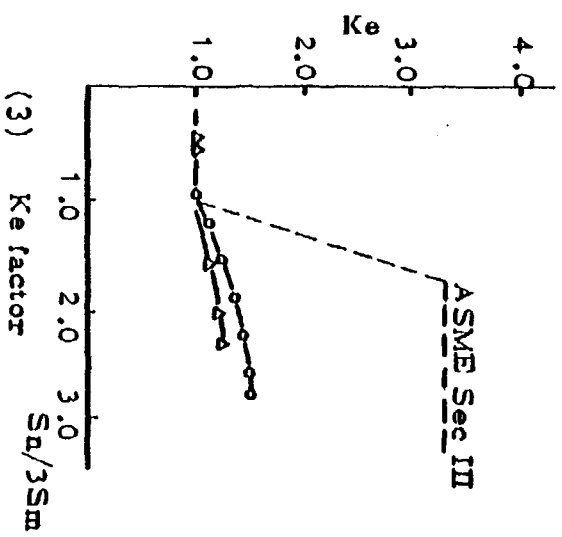
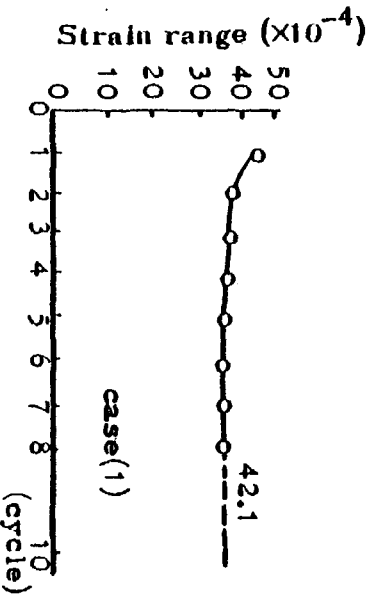
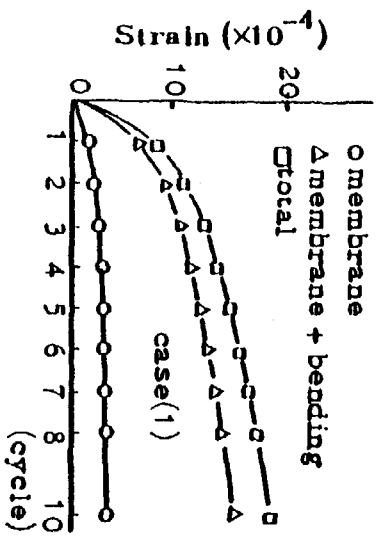


Fig. 14 Results of Non-linear analyses

Table 1. Test conditions for plate specimens

Strain range (elastic)	Temperature	Room	500°C	550°C	600°C
1.0%		TP .No .14 TP .No .13	TP .No .8	TP.No .10	TP .No .7
0.7%		-	-	TP .No .11	-
0.5%		-	-	TP .No .9	-
0.4%		-	-	TP .No .4	-
0.3%		-	-	TP .No .12	-

loading cycle condition (zero-tension)

Table 2. Test conditions

No.	Initial Temp. (°C)	Range of ΔT	ΔT	Load
1-6	100	25	(0-25)	Low Temp.
	-300	-60	(0-60)	Elastic
10-1 10-2	550	160	0 -160	+
11-1 11-11	550	250	0 -250	+
12	550	330	-30 -250	=
13	550	365	-115 -250	=
14	550	300	0 -300	+
15-1 15-5	550	380	-130 -250	=
16-1 16-5	550	400	-150 -250	=

(Remark) Test No. 12, for example, shows that the value of shed temp. minus plate temp. varies from -30°C to 250°C and the temperature range is 330°C.

Table 3. Stress calculated by elastic analysis

Test 6	$\Delta T = 52^{\circ}\text{C}$	$S_n = 10.9 \text{ kg/mm}^2$	$S_n' = 5.8 \text{ kg/mm}^2$
Test 11	$\Delta T = 250^{\circ}\text{C}$	$S_n = 49.4 \text{ kg/mm}^2$	$S_n' = 26.3 \text{ kg/mm}^2$
Test 16	$\Delta T = 400^{\circ}\text{C}$	$S_n = 79.4 \text{ kg/mm}^2$	$S_n' = 42.1 \text{ kg/mm}^2$

Table 4. Progressive deformation of shroud to tube sheet junction

Detail Inelastic Analyses

Case 1	0 - Tension $S_n = 61.2 \text{ kg/mm}^2$
2	0 - Tension $S_n = 47.0$
3	0 - Tension $S_n = 32.9$
4	Tension-Compression $S_n = 100 \text{ kg/mm}^2$ w/o Creep
5	Tension-Compression $S_n = 100 \text{ kg/mm}^2$ W Creep
6	0 - Tension $S_n = 62 \text{ kg/mm}^2$ 450°C
7	Same as Case 1 with Cyclic Stress Strain Relation

Results

Cases 1, 2, 3, 6	Small progressive Strain
Cases 4, 5, 7	Shake Down